The Influence of Road Network Topology on Street Flooding in New York City—A Social Media Data Approach

by

Chen Zuo

A thesis submitted
in partial fulfillment of the requirements
for the degree of
Master of Science / Master of Landscape Architecture
(Environment and Sustainability)
in the University of Michigan
04 2023

Thesis Committee:
Assistant Professor Runzi Wang, Chair
Associate Professor Drew Gronewold
Assistant Research Scientist Yi Hong*

ABSTRACT

Road network is important in urban planning because it not only shapes the spatial structure of an urban area but also serves as a critical stormwater infrastructure. Existing literature on urban flooding focused on flood risk assessment, traffic disruption, and congestion analysis at large river basin scales under high-magnitude and high-intensity flooding events. However, the relationship between road network topology and urban flooding remains unclear. Additionally, smaller, and more frequent street flooding events, which cause higher cumulative costs, are often less studied. The common use of physically-based hydrological models with strict data requirements further limits the scope of previous flooding studies. To address these gaps, this study utilized statistic models to investigated the influence of urban road network topology on street flooding risks in 557 sewer catchments across New York City (NYC) with a social media big data approach. We used 11 road network topology metrics and 11,042 street flooding complaints recorded on the NYC 311 Sewer Complaints platform from 2010 to 2022. We performed generalized linear mixed models to investigate the relationship between road network topology metrics and street flooding risks. The control variables included sewer drainage type, rainfall intensity, land use, impervious density, human and nature factors. We found that road network connectivity significantly affected the risk of street flooding, while the influence of impervious was not significant. Our findings suggested that increasing road network connections, average road width, and number of intersections while decreasing the total road length, total number of roads, and sewer catchment area would reduce the risk of street flooding. Therefore, optimizing road network connectivity is a key consideration for flooding mitigation in urban planning.

Keywords: road topology, urban flooding, road connectivity, social media, mixed model

TABLE OF CONTENTS

Chapter 1 Introduction

Urban flooding caused significant disruption to cities' services, including energy and water provision, transportation, and housing (X.-Z. Chen et al., 2015; Hammond et al., 2015; Hoekstra et al., 2018; Schaeffer et al., 2012). It is the natural hazard with the most significant economic and social impact in the United States, and these impacts are becoming more severe over time (Medicine et al., 2019). As climatic uncertainty increases, one of the more common weather-related hazards is small-scale urban flooding (e.g., street flooding) which needs attention (Rosenzweig et al., 2018). Existing research on urban flooding focused mainly on high-magnitude and high-intensity events at the large river basin scale. However, smaller and more frequent street flooding events might have a higher cumulative cost (Moftakhari et al., 2018). Especially in urban areas with high population density, the consequences of street flooding were often more severe than those of coastal or tidal flooding events (Hammond et al., 2015). Because the definition of street flooding is unclear in current studies, it was necessary to establish a clear definition. Our definition of 'Street Flooding' is based on the definitions provided by the European Standard EN 752 (CEN, 1996) for 'Flooding', the definition of 'Nuisance Flooding' (Moftakhari et al., 2018), and the definition of 'Pluvial Flooding' (Hammond et al., 2015). Specifically, we define 'Street Flooding' as a scenario where small-scale and high-frequency surface flow is incapable of being absorbed by a drainage or sewer system, thus causing water to accumulate on the street surface during rainfall.

The impact of flooding on road networks and traffic systems has received significant research attention in recent years (Britain & Brown, 2014). Several studies over the last decade have investigated weather impacts on the road network, including topics of flooding disaster measures, road systems management strategies, and road system's adaptation to flooding disasters (Hammond et al., 2015; Kadaverugu et al., 2021; Kramer et al., 2016). However, existing research assessing the impact of flooding on the road did not capture the complexity of their interactions (Pregnolato et al., 2017), especially the possibility of two directions exchanges between the sewage network and the street, quantifying the influence between the road network and urban flooding is thus particularly complicated (Paquier & Bazin, 2014). Currently, research studying road networks' influence on flooding focused on (1) Small-scale studies of road junction morphology's influence on surface runoff using a hydrological model. For example, studies used improved one or two-dimensional modeling of the street flows through the virtual network with several morphology crossroads (Lipeme Kouyi et al., 2010; Pons, 2010); (2) Simulation of flow distribution in the road network. Studies investigated surface flow complexity at the crossroads, modeled surface flows during urban floods, and assessed the flow distribution within the street network (S. Lee et al., 2016; Paquier & Bazin, 2014). Researchers also explored the small-scale features of road networks (e.g., curb height, road camber shape, dimensions) and road connectivity that played a crucial role in transporting water in flooded areas (de Almeida et al., 2018); (3) Large-scale study on road density's influence on flooding. Studies on this topic concluded that higher road density in urban development led to more inland flooding (Li et al., 2022; Rahman et al., 2021). Summarizing existing research, we found road density was closely related to runoff and drainage process in a floodplain (Kalantari et al., 2014; Rahman et al., 2021), but there was little research investigating the impact of the road network topology (RNT) on flooding, especially at city scale.

Although the roles of road networks have become more important with the advancement of urban flooding research, the uncertainty of flood modeling and the data acquisition and quantification of street flooding remained challenging (Dottori et al., 2013; Merwade et al., 2008; Paquier & Bazin, 2014). For

instance, flooding model establishment required detailed information on road and sewer network structure and surface area characteristics, which were often unavailable and confidential. Some research has developed a novel approach to generate a hydraulic sewer model with minimal data, but it had limitations such as biased diameter distribution estimation and exclusion of storage facilities (Blumensaat et al., 2012). Furthermore, due to the limitation of data precision, those data did not represent small-scale urban surface features and their influence on flooding distribution (Fewtrell et al., 2011; Neal et al., 2011; Schubert & Sanders, 2012). Statistical and data-driven methods, which are computationally cheaper and more efficient, have gained popularity in past decades in modeling urban flooding (Cox et al., 2002; Fowler et al., 2007; Lu et al., 2016). Social media big data is a promising alternative to overcome the difficulty in obtaining street flooding data (Wang, 2018). The traditional methods to obtain street flooding data usually had low spatial resolution and coverage. The application of satellite imagery and aerial photography was limited by vegetation canopies and cloud cover during floods (Wang et al., 2018). Radar was unable to extract flood data from urban areas because of the corner reflection principle associated with coarse ground resolution (Wilson et al., 2007). There were also insufficient sensors on the streets used for urban flood monitoring purposes (Wang et al., 2018). Therefore, the social media big data approach relying on volunteer reports from citizens could be a potential solution to provide primary or complementary urban flooding data. For example, NYC 311 sewer complaints data could be accessed via the NYC Open Data website, where data are available from January 2010 to now. With the time, date, and exact location of a flooding complaint, the 311 street flooding complaints serve as a valuable tool for urban flooding model validation. Data provided by 311 could also be applied to understand the causes and effects of street flooding (Agonafir et al., 2022).

This study aimed to explore the impact of road network topology on street flooding risk by investigating the associations between urban road network topology metrics and street flooding social media data using generalized linear mixed models (GLMMs). Our hypothesis was that an unreasonable road network leads to sewer backup, man-hole overflow issues, and blockages in stormwater underdrains, all of which contributed to street flooding. Additionally, we drew hydrological implications and suggested urban planning solutions based on the regression results. Our research questions were as follows: (1) What is the spatial and temporal distribution of street flooding events in New York City? (2) What are the most important road network topology factors that affect street flooding risk in New York City, and what is their influence? (3) Do the effects of road network topology factors on street flooding risk vary based on different drainage and rainfall types?

Chapter 2 Study Site and Materials

2.1. Study Site

Our study site NYC has an area of 778.2km^2 and the annual rainfall of 1,270 mm (NWS, 2020d). Because 72% of NYC is covered with impervious surfaces (*The Impact of Investing - NYW*, n.d.), it is susceptible to flood hazards. Due to the high intensity residential and commercial development, there is a huge damage to life and property from urban flooding (Maantay & Maroko, 2009). According to the New York State Climate Hazards Profile, NYC has experienced between 90 and 102 severe storms between the years 1960 through 2014, and the subsequent damage costs ranged between $4 to $17 million (State of New York, 2020).

We examined 557 drainage catchments in NYC (Figure 1) and categorized them into two types of drainage systems: combined and separate. We excluded Staten Island from the study due to input data errors. Combined drainage systems, which are predominantly found in historical areas like Manhattan, Bronx, and parts of Brooklyn and Queens, make up approximately 85% of the study area. The remaining area uses separate drainage systems, which are primarily found in newer and low-lying areas such as southeast Queens, south Brooklyn, and Staten Island (*Sewer System - NYC DEP*, n.d.).

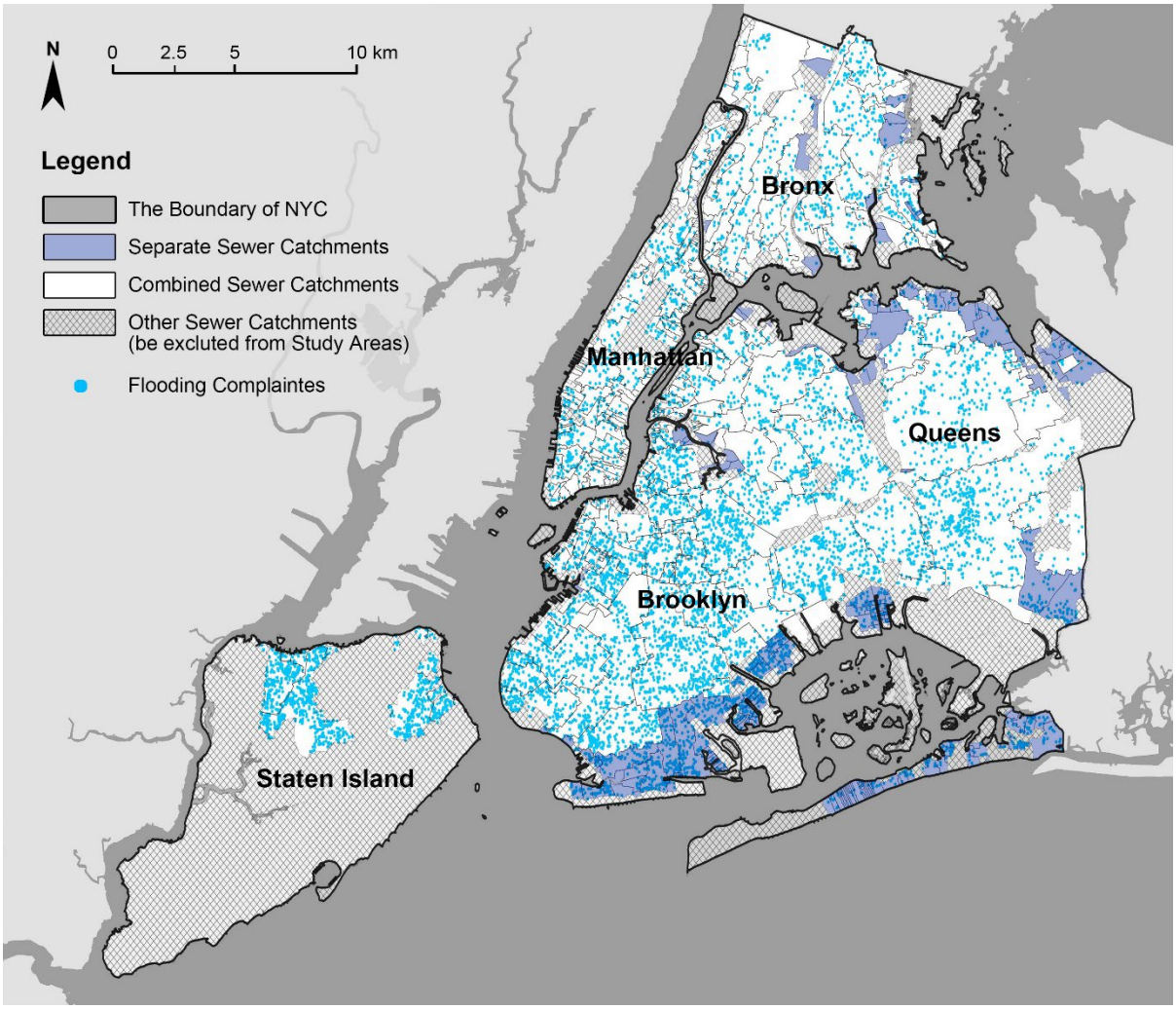

Figure 1. NYC drainage catchments with drainage systems types and flooding complaints

2.2. Data and Variables

Raw data we used in this study included 311 NYC sewer complaints, hourly precipitation, road network shapefile, Digital Elevation Model (DEM), catchments boundary shapefile, drain inlets shapefile, impervious surface, land use, NDVI, and NDWI (as detailed in Table 1).

Table 1. Data sources

Data	Format	Resolution	Time	Source
Street Flooding Complaints	Text	Point	2010-01-01 to 2022-04-28	311 Service Requests from 2010 to Present
Hourly precipitation	Text	Hourly	2010-01-01 to 2022-06-01	NOAA Climate Data Online
Road Network	Shapefile	Line	2022-08-30	NYC Street Centerline (CSCL)
Digital Elevation Model	Raster	1ft	2018-09-10	1-foot Digital Elevation Model
Storm Sewer System	Shapefile	Polygon	2018-08-01	Municipal Separate Storm Sewer System (MS4) Data
Drain Inlets	Shapefile	Point	2021-12-30	NYCDEP Citywide Catch Basins
Impervious Shapefile	Shapefile	Polygon	2020-08-06	DEP's Citywide Parcel-Based Impervious Area GIS Study
Land Use	Shapefile	Polygon	2022-11	NYC GIS Zoning Features
NDVI	Raster	30m	2013-01-01 to 2019-12-31	Landsat 8 Collection 1 Tier 1 Annual NDVI Composite
NDWI	Raster	30m	2003-04-07 to 2019-12-31	Landsat 8 Collection 1 Tier 1 32-Day NDWI Composite

The road network topology metrics, including the layout, geometry, and spatial pattern of the road network, were the independent variables in this study (M G et al., 2021). In graph theory, the topology relationship is analyzed through topology associated with the position and relationship between points, lines, and areas (Porta et al., 2006). In this study, the connectivity of the road network was indicated using the Alpha, Beta, Gamma, and Theta indices (Table 2.), which were derived from the graph theory (Kansky, n.d.). The remaining independent variables, namely network density, intersection density, and ETA, were not related to graph theory but could also be used to describe the connectivity.

To enhance the internal validity of the relationship between road network topology and street flooding and limit the influence of confounding and extraneous variables that could affect street flooding, we included several control variables in our study, including sewer drainage type, social attributes, land use, NDVI, NDWI, and impervious surface density. According to recent studies, the impact of sewerage systems on flooding varies depending on the type of system. While both separate and combined

sewerage systems can experience flooding during extreme conditions, combined systems are more prone to overflows issues. Separate sewerage systems are often considered a solution for receiving water pollution problems of combined systems (Carleton, 1990). Recently, research on the implications of land use change on hydrological processes has gained significant prominence (Y. Chen et al., 2009; Fox et al., 2012; Zope et al., 2016). Additionally, investigations into the social factors contributing to flooding have also become an important focus (Ding & Wei, 2022; Zhang et al., 2021). Furthermore, natural factors such as NDVI and NDWI have been identified as significant factors influencing flooding research (Ahmed & Akter, 2017). We also included rainfall intensity as control variable in this research. We identified two years as the return period threshold and classified rainfall events with an intensity greater than the two-year return period rainfall (90th percentile) as 'Heavy' rainfall events and the rest as 'Normal&Light' events.

Table 2. Independent and Control Variables

Parameter	Formula*	Description	Range
Alpha	(e-v+1)/(2v-5)	Number of essential circuits to maximum probable circuits in the sewer catchment	0 to 1
Beta	e/v	Number of links to number of nodes in the sewer catchment	≥0
Gamma	e/(3(v-2)	Actual count of links to maximum number of links in the sewer catchment	0 to 1
ETA	ΣL/e	Indicates average link length of network (Kansky, 1963) in the sewer catchment	≥0
Theta	ΣL/v	Network length to number of nodes in the sewer catchment	≥0
Intersection Density (per sqm)	ΣI/A	Describes the intersections per unit area (Cervero and Kockelman, 1997) in the sewer catchment	≥0
Network Density (m per sqm)	ΣL/A	Designates the network length per area (Bento et al., 2003) in the sewer catchment	≥0
Road Mean Grade	$\Sigma(H_i/L_i)/i$	The mean grade of all roads in the sewer catchment, where H_i indicates the slope and L_i indicates the horizontal length of road from road '1' to road 'i'	0 to 1
Road Mean Width (m)	$\Sigma W_i/i$	The mean width of all roads in the sewer catchment, where W_i indicates the width of road from road '1' to road 'i' and 'i' is the total number of roads	≥0
Road Mean Elevation	$\Sigma E_i/i$	The mean elevation of all roads in the sewer catchment, where E_i indicates the elevation of road from road '1' to 'i' and 'i' is the total number of roads	≥0

Sewer Drainage Type		The types of sewer drainage catchment: Combined drainage system, Separate drainage system	
Sewer Areas (sqm)	A	The area of sewer catchment	≥0
Drain Inlets Density (num per sqm)	Drain Inlets Number/A	The total number of drain inlets in the sewer catchment	≥0
Population Density	Population/A	The total number of people in the sewer catchment	≥0
Commercial Land Use Percentage	Land Area/A	Commercial districts	0 to 1
Park Land Use Percentage	Land Area/A	Public Parks districts	0 to 1
Residence Land Use Percentage	Land Area/A	Residence districts	0 to 1
Manufacturing Land Use Percentage	Land Area/A	Manufacturing districts	0 to 1
NDVI		Normalized Difference Vegetation Index, to determine the density of green on a patch of land (GISGeography, 2017)	-1 to 1
NDWI		Normalized Difference Water Index, to determine the plant water content (Gao, 1996)	-1 to 1
Impervious Percentage	Area of impervious/A	The percentage of pavements that are covered by water resistant materials in a given area (*Remote Sensing of Impervious Surfaces*, n.d.)	0 to 1
Rainfall Intensity Type		The types of rainfall Intensity: Heavy rainfall, Normal&Light rainfall	

*Note of Table 2: * 'e' is the number of edges, 'v' is the number of vertices, 'L' is the road link length in m, 'I' is the count of intersections, 'A' is the area of catchment.*

The dependent variable was street flooding risk. The street flooding information was retrieved from the NYC 311 platform from January 1, 2010 to April 28, 2022, resulting in 303,849 street flooding complaints. After conducting a trial to match rainfall events with street flooding complaints, we were able to classify the complaints into three categories and train a Random Forest Classification model to classify the dataset. This process resulted in the keeping of only 11,042 complaints that could be attributed to runoff and overflow from the urban drainage system during rainfall events. We utilized logistic regression to predict the probability of events occurring. The original street flooding complaints in the NYC 311 data were labeled as 'True' reports, and we generated 'False' reports for catchments that did not have complaints during each rainfall event. As a result, the regression analysis included

356,461 samples from 557 catchments and 630 rainfall events, with 11,042 labeled as ‘True’ and 345,419 as ‘False’.

Chapter 3 Methodology

Our methods included three steps: data preprocessing, clustering road network patterns, and regression modeling (Figure. 2). In the data preprocessing, we cleaned 311 NYC complaints and abstracted various indices and metrics from the raw dataset, and implemented K-means clustering analysis to investigate road network topology characterizers of different sewer catchments. ANOVA test was conducted to compare and select GLMM regression model, and then GLMM regression analysis was performed. The regression results were used to suggest road network planning methods. All methods were implemented using RStudio (Version 4.1.2) and ArcGIS Pro (Version 2.7.0).

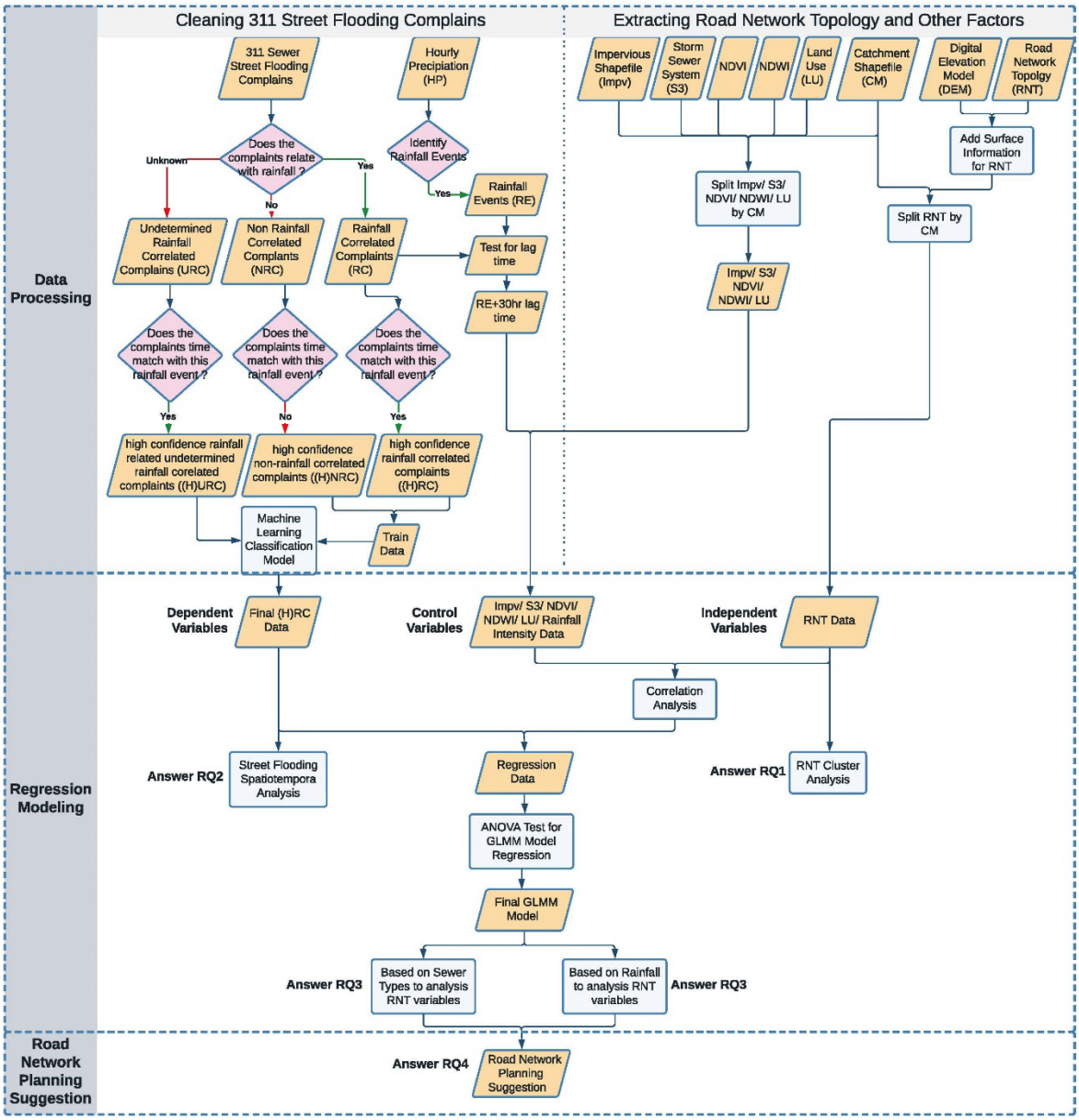

Figure 2. Method framework

3.1. Generating Street Flooding Complaints and Road Network Topology Datasets

The street flooding complaint data was divided into three sets: rainfall-correlated complaints (RC), non-rainfall-correlated complaints (NRC), and undetermined rainfall-correlated complaints (URC). The RC

data had a small sample size and was clustered in a few catchments, so we cleaned NRC and URC data with the help of rainfall event data to select NRC and URC with high confidence in correlation with rainfall events. Based on the possibility of a time lag between the occurrence of a rainfall event and its subsequent report, we matched street flooding complaints with rainfall events, varying the lag time between 1h to 72h. 30h was determined to be the appropriate lag time to indicate that street flooding complaint was correlated with a rainfall event. High confidence rainfall-correlated complaints ((H)RC), high confidence non-rainfall-correlated complaints ((H)NRC), and high confidence undetermined rainfall-correlated complaints ((H)URC) were included as the final complaints dataset after matching with rainfall events. A Random Forest Classification model was trained using (H)RC and (H)NRC as training labels to classify (H)URC dataset. At last, we had 11,042 high confidence rainfall-correlated complaints.

To calculate road network topology metrics, we utilized several datasets, including road network, DEM, and storm sewer system. We excluded features of highways, overpasses, and pedestrian trails from the road network data due to the missing of elevation information. We calculated road network topology factors for each sewer catchment as the independent variable in the regression model together with control variables such as land use, impervious area percentage, NDVI, and others.

3.2. K-means Clusters Analysis of Road Network Topology

To investigate road network topology characteristics of different sewer catchments, we implemented a K-Means clustering analysis with 11 explanatory variables to categorize sewer catchments to several clusters with a notable difference in road network topology. Cluster analysis can help to group similar properties together based on their characteristics and provide a more structured way of analyzing the data (Edwards & Cavalli-Sforza, 1965). K-Means clustering can divide objects into k clusters so that the level of similarity between members in one cluster is high, while the level of resemblance to the members in the other cluster is low (Dubey et al., 2018). We performed K-means clustering on 551 catchments with 11 road network topology variables and determined the optimal number of clusters based on the elbow method. We examined the RNT characteristics and the spatial distribution of different clusters. We also analyzed the street flooding distribution by month and clusters. Then, we compared the mean and standard deviation regarding the distribution of the clusters for important RTN variables. By examining the loadings of each variable on each dimension, we identified variables that explained the highest variance within the road network topology data. We plot the data in the space of these two components and examine the emerging road network topology characteristic.

3.3 Regression Models to Establish Connections Between Road Network Topology and Street Flooding Risk

To analyze the relationship between selected road network topology metrics and street flooding, we utilized the Generalized Linear Mixed Model (GLMM) approach. The selected topology metrics were chosen based on correlation analysis to remove some highly correlated metrics. Street flooding is the result of a complex flow mechanism affected by direct and indirect influence from sewer system, road network topology, rainfall intensity, land use, nature factors, human active and interaction factors. Although we added these factors in the regression model, it was not possible to include all the factors influencing the street flooding over time, space, and individuals. To reduce the bias parameter estimation caused by the unobserved factors, we used mixed effects models (also known as random parameter models) to allow some unknown parameters to vary across sewer catchments and rainfall events rather than fixed in traditional models (Guo et al., 2017).

Eq. (1) describes the GLMM regression formula:

$$\Pr(y_i = 1|X_i) = \int \Phi(X_i\beta) \cdot f(\beta|\varphi)d\beta = \int \left(\frac{exp(X_i\beta)}{1 + exp(X_I\beta)}\right) \cdot f(\beta|\varphi)d\beta \quad (1)$$

where

Pr = probability of the risk (y_i) of street flooding observation i,

β = vector of regression coefficients,

X_i = vector of explanatory variables for street flooding observation *i*, and

Φ = cumulative distribution function of logistic distribution.

$f(\beta|\varphi)$ = the density function of random parameter β with distribution parameter φ.

In the regression, the total number of street flooding complaints, including "True" and "False", was 356,461. The random effects included 557 sewer catchments and 630 rainfall events matched with street flooding complaints. Furthermore, to compare models with different independent, control, and interaction variables, ANOVA tests for model selection were applied. A total of 34 models were compared, and the final model was selected. The final models' independent variables included Alpha, Beta, Theta, Road Mean Width, and Intersection Density. The control variables consisted of Sewer Type, Sewer Area, Residence Land Percentage, NDVI, and Rainfall Intensity Type. Additionally, interaction variables were considered, including Alpha : Sewer Type, Beta : Sewer Type, Theta : Sewer Type, Road Mean Width : Sewer Type, Sewer Area : Sewer Type, Alpha : Rainfall Intensity Type, Beta : Rainfall Intensity, and Theta : Rainfall Intensity.

Chapter 4 Result and Discussion

4.1. Patterns of Street Flooding Complaints and Road Network Topology

By investigating the locations of street flooding complaints reported between January 2010 and April 2022 (Figure 3 (a)), we found the number of flooding complaints was highest in Staten Island, Brooklyn, and lower Queens, while the outer districts of Brooklyn, Queens, and lower Manhattan had the highest complaint density. Conversely, the frequency of complaints in the inner districts and Bronx was lower, indicating a spatial clustering effect of street flooding complaints. Also, we mapped the hotspot of flooding complaints over a 12-year period by month and the temporal trend of the locations of these complaints represented by longitude and latitude (Figure 3 (b)). The spatiotemporal patterns of street flooding indicated that (1) most complaints occurred in late spring and summer, which the mechanism could be flooding caused by convective storms and tropical cyclones (B. Smith & Rodriguez, 2017). Previous research also suggested that the majority of street flooding complaints were affected by heavy rain events, and precipitation is the primary driver of street flooding in NYC (Agonafir et al., 2022); (2) street flooding complaints shifted primarily from the northeast to the southwest during the winter, which agreed with the clear seasonal pattern of rainfall in the NYC influenced by the complex spatial relationship between land and waterbody in the area (Smith & Rodriguez, 2017; Yeung et al., 2011).

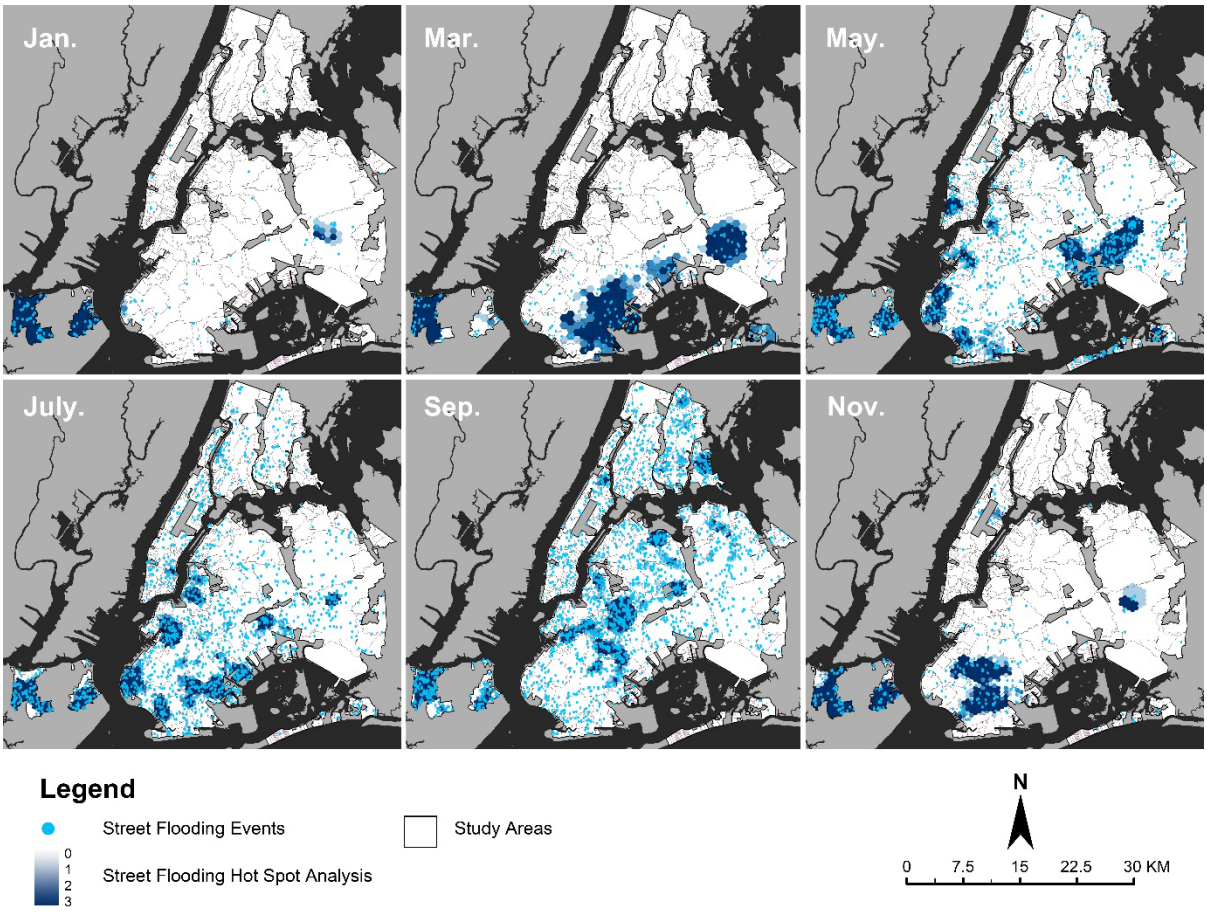

(a)

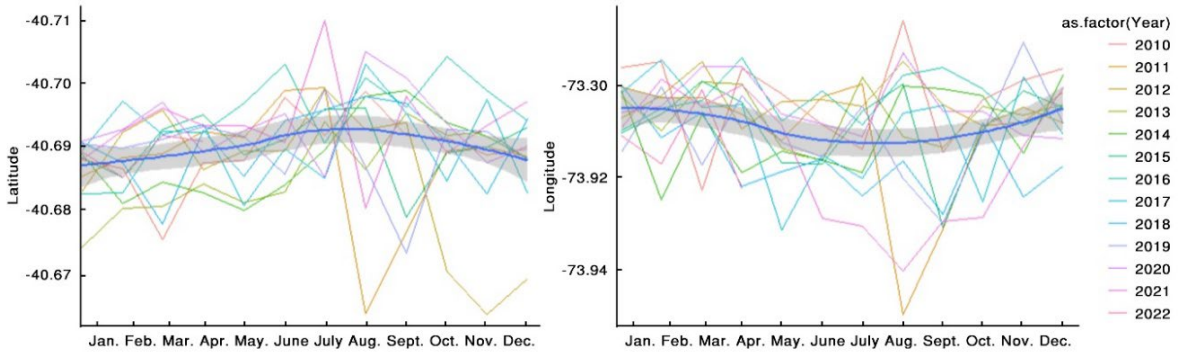

(b)

Figure 3. (a) The hotspot maps of street flooding complaint from 2010 to 2022. (b) The location pattern of street flooding complaint by month from 2010-2022.

The 551 NYC catchments were divided into 7 distinct clusters according to the road network topology. We tested the number of clusters from 1 to 10 and selected 7 as the optimal number of clusters according to the elbow method (Figure 4 (a)). We summarized the characteristics of each cluster by plotting the histogram of each RNT variable by cluster group. The dominant clusters were Clusters 2, 5, and 6. Cluster 2 comprised 15 catchments mainly located in central areas with higher elevation, larger average catchment areas, and greater connectivity of road networks than other clusters. Cluster 5 included 183 catchments primarily located in coastal regions with lower elevations, small average catchment areas, and high road network density. Cluster 6 included 212 catchments located mainly in coastal areas with

small sizes, low road network connectivity, and high road density. Clusters 1, 3, 4, and 7 had 14, 73, 55, and 5 catchments respectively with different combinations of characteristics of catchment size, road density, elevation.

We plot the street flooding complaints density over a 12-year period categorized by clusters (Figure 4 (b)). We found a clear seasonal variation of the complaint's density in all 7 clusters, with a higher complaint's density during summer and early fall and a lower density during late autumn to early spring. Nonetheless, certain sewer catchments were found to be more prone to flooding based on complaint distribution by cluster and month. Specifically, clusters 1 and 6 exhibited higher monthly average complaints density compared to other clusters. Furthermore, while clusters 4, 5, and 6 showed stable seasonal variation in the complaint's density, clusters 1 and 7 displayed a relatively unstable seasonal variation. In summary, significant differences in flooding density existed among different clusters and across different months.

Our analysis highlighted the complex spatiotemporal patterns of street flooding and their clustering effects. This information can be used to find flooding hotspots spatially and temporally, as well as understand the associated catchment characteristics. It can further inform policies and infrastructure improvements to mitigate the impact of street flooding on vulnerable communities, as well as propose flooding adaptation strategies.

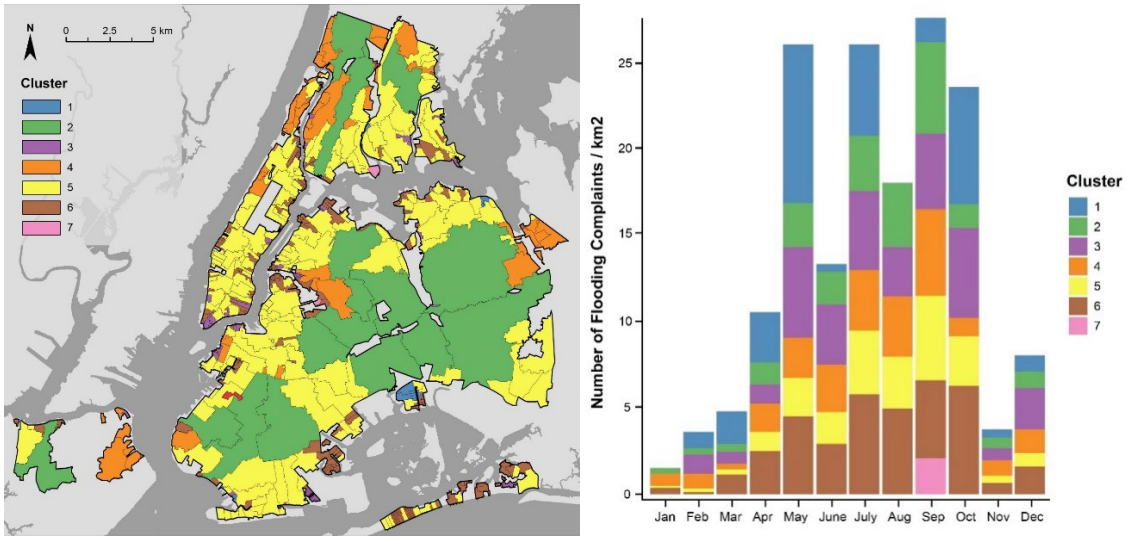

(a) (b)

Figure 4. (a) sewer catchment cluster map. (b) street flooding complaint distribution by month and clusters

4.2. Important Road Network Topology Variables Influencing Street Flooding Risk

Our finding demonstrated that road network topology was a crucial factor in determining the risk of street flooding. In contrast, the percentage of impervious areas did not significant impact the flooding risk. Using ANOVA, we selected a final model that included ten main effect variables and eight interaction effect variables. The results indicated that all road network topology variables and interaction variables were statistically significant ($p<0.05$) (Table 3). Beta, Theta, and Sewer Area increased the street flooding risk, while Alpha, Mean Road Width, and Cross Density decreased it. Additionally, Beta, Theta, and Alpha of the road network were the most significant topology metrics. We observed that higher physical connectivity of the road network, as indicated by a higher Alpha,

resulted in a decreased street flooding risk. Furthermore, road networks with a higher number of intersections, as indicated by a lower Beta and Theta, also reduced the street flooding risk.

Table 3. GLMM Regression Results

Predictors	Estimate	Confidence interval	*p*-value
(Intercept)	-3.489	-5.194~ -1.784	<0.001***
Alpha	-4.119	-5.328~ -2.910	<0.001***
Beta	5.199	3.916 ~ 6.483	<0.001***
Theta	1.390	1.047 ~ 1.734	<0.001***
Mean Road Width	-0.426	-0.623 ~ -0.229	<0.001***
Intersection Density	-0.461	-0.737 ~ -0.185	0.001**
Sewer Area	0.582	0.437 ~ 0.728	<0.001***
Residence Density	0.637	0.469 ~ 0.806	<0.001***
NDVI	-0.612	-0.793 ~ -0.431	<0.001***
Rainfall Normal&Light	-3.573	-5.273 ~ -1.874	<0.001***
Drainage Type Separate	0.562	0.160 ~ 0.964	0.006**
Alpha : Drainage Type Separate	1.087	0.065 ~ 2.114	0.037*
Beta : Drainage Type Separate	-1.472	-2.547 ~ -0.396	0.007**
Theta : Drainage Type Separate	-0.548	-0.922 ~ -0.174	0.004**
Sewer_Area : Drainage Type Separate	2.562	1.445 ~ 3.679	<0.001***
Mean Road Width : Drainage Type Separate	0.404	0.083~ 0.726	0.013*
Alpha : Rainfall Normal&Light	1.613	0.691 ~ 2.535	<0.001***
Beta : Rainfall Normal&Light	-1.856	-2.890 ~ -0.823	<0.001***
Theta : Rainfall Normal&Light	-0.675	-0.897 ~ -0.454	<0.001***
Observations		356,461	
Marginal R^2		0.612	
AUC		0.91	

While significant in this study, the importance of road network structure has been largely undermined in the existing literature. Previous research showed that urbanization exacerbated flood risk through the expansion of impervious surfaces that prevented water from infiltrating the soil and caused more runoff to overwhelm storm drainage systems (Chang & Franczyk, 2008; Hailegeorgis & Alfredsen, 2017). Recent studies reported that connected impervious area (i.e., surfaces that contribute directly to runoff in a storm network or stream) was a better indicator of hydrologic response, stream alteration, and water quality than total impervious area (Sytsma et al., 2020). Because urban watersheds, lined with impervious surfaces, have a limited amount of infiltration and recharge during heavy rainfall; thus, surface flow dominates the hydrological response (Serrano & Serrano, 2010). We argued that road network topology influenced street flooding essentially because road systems are the preferential path for surface runoff (Singh et al., 2018). Changes in surface flow network and runoff conveyance

characteristics associated with road network topology influenced flooding risk in urbanized catchments (J. A. Smith et al., 2002; Turner-Gillespie et al., 2003; Wolff & Burges, 1994). Also, the layout of the storm drainage system was closely related to the road network (Jia et al., 2019; Mair et al., 2017). Therefore, it was reasonable that road network topology variables significantly influenced street flooding risk.

Alpha Index, which was negatively correlated with street flooding risk, reflected the number of closed circuits in a network. The higher the number of closed circuits, the higher the Alpha Index (Freiria et al., 2015). When the road network became less physically connected, as indicated by a lower Alpha, the risk of street flooding increased. It was found the effect of pipe network structures on runoff was higher in the branched networks, of which water flow is one-directional and tends to concentrate at the catchment outlet. Contradictory, In the looped networks where runoff paths are multi-directional, runoff could be routed to several alternative water paths, resulting in reduced peak runoff (J. Lee et al., 2018). Similar mechanisms have been used for overflow regulations designed with flow diversion (Moffa, 1997).

Beta and Theta were positively correlated with street flooding risk, where Beta was defined as the number of paths passing through a vertex (Freiria et al., 2015), and Theta represented the total path length passing through a vertex. Lower Beta and Theta indicated a higher number of intersection when controlling the number of paths and total length of path. Further, Beta and Theta can be explained as drainage inlet density and flow distance in urban hydrology, both influencing drainage efficiency. After analyzing the spatial relationship between drainage inlets and road intersection, we found 86.97% drainage inlets were in the buffer areas of road intersection. A higher density of drainage inlets can help reduce street flooding risk by increasing the chances surface water enters the drainage system because drainage inlets are pivotal interfaces between surface and subsurface drainage systems (Butler & Memon, 1999). Previous research also confirmed that runoff efficiency depended upon inlet density, grate type, gutter flow, road geometry, as well as the hydraulics of the approaching flow (Gómez & Russo, 2011). Decreasing Beta and Theta was particularly important in areas with high rainfall intensity or areas with flat topography where surface water runoff can accumulate quickly.

4.3. Effect of The Interaction Effects Between Road Network Topology, Drainage System, and Rainfall

According to the interaction effects between road network topology, drainage system type, and rainfall type (Figure 5), we found that in the combined sewer catchment, high Beta and Theta led to greater street flooding risk compared to a separated sewer system. This is possible because combined drainage catchments always had higher population density, older age of sewer infrastructure, and lower capacity of drainage than separate drainage catchments (Moffa, 1997). 80% area of NYC relies on the combined drainage system, which is mostly found in older areas, such as Manhattan, Bronx, and parts of Brooklyn and Queens. The separate drainage catchments are typically in newer areas, such as southeast Queens and south Brooklyn (Figure 1). Because of the limited drainage capacity of combined drainage catchments, the drainage system connectivity indicated by road network topology could be more important in decreasing street flooding risk. Moreover, the combined drainage catchments were primarily located upstream, while separate drainage catchments were mostly located downstream. Pipe diameters in the upstream areas were usually smaller than the lower areas of the network, and therefore, the flow capacity of separate drainage systems was higher than the combined drainage system in NYC.

As a result, the effect of road network topology in separate drainage catchments was less significant due to the higher sewer capacity.

We also found Beta and Theta had less influence on street flooding risk during normal and light rainfall compared to heavy rainfall events. When extreme rainfall events produced high surface runoff rates flowing along preferential pathways, including roads, footpaths, natural ground depressions, and small water courses, surface runoff cannot be efficiently conveyed into the underground drainage system (Russo et al., 2021). The limited capacity of the drainage system during extreme rainfall could result in sewer flow back to the catchment surface (Maksimović et al., 2009).

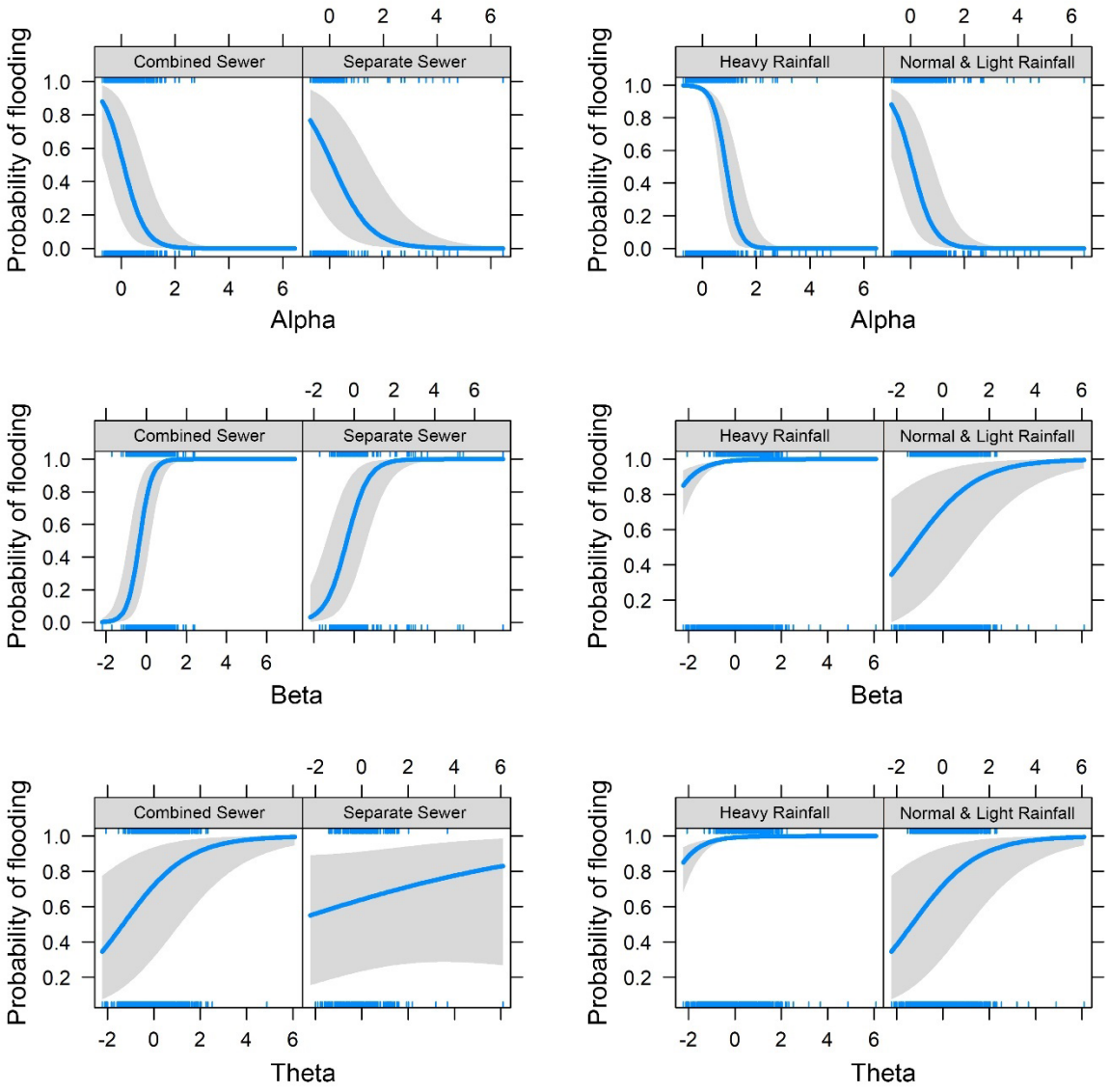

Figure 5. The regression estimate of Alpha, Beta and Theta based on different drainage systems and rainfall events.

4.4. Road Network Planning Suggestions from Road Network Topology Perspective

- Improving Road Network Connectivity

The structure and dynamics of road network considerably influenced the risk of street flooding, where increasing road network topology connectivity (represented by Alpha) is important. We found several

hotspot areas with low road network topology connectivity, such as the central area of Manhattan, the northern part of Queens, the coastal areas of Brooklyn and Bronx, and the entire Staten Island. To improve road connectivity and the associated pipe facility connectivity in these areas and the future new urban areas, we suggest several planning strategies (Figure 6): (1) Reducing the number of dead-end roads and connecting them with the surrounding road systems; (2) Increasing the number of loops in the road network; (3) Enhancing the road network topology connectivity between adjacent catchments; (4) Removing redundant roads from the network. Implementing these suggestions can enhance the performance of the pipe system by improving the road network's connectivity.

- Increasing the Number of Intersections

Increasing the number of road intersections can increase the density of drainage inlets density and improve the efficiency of runoff flowing to a drainage system. We found a considerable difference in intersection density between different catchments in NYC, which could be attributed to varying development phases, zoning, and land use planning. The connectivity of stormwater infrastructure between different zones was also low. Therefore, we suggest (Figure 6): (1) Road infrastructure planning should improve the connection between different zones to improve the average capacity; (2) Avoiding multiple roads intersecting at the same intersection and decomposing such intersection into multiple crossroads; (3) Achieving a more balanced spatial distribution of the road intersections.

- Shrinkage Total Length of Road Network while Controlling Road Network Topology Connectivity

Optimizing road network design by reducing total road length can have multiple benefits, such as reducing surface flow duration, enhancing runoff efficiency, and minimizing unnecessary infrastructure investment. The distribution of average road lengths in various catchments in NYC was quite uneven, with considerably higher average road lengths in Staten Island, midtown Manhattan, central Brooklyn, and southern Queens' catchments, which might be attributed to different zone functions, development periods, and land use types. To achieve a shorter road length while maintaining similar connectivity levels, we recommend (Figure 6): (1) Avoiding meandering road designs. (2) Improving public transportation to enhance travel efficiency and achieve similar transportation capacity with shorter road lengths.

- Decreasing Number of Roads while Controlling Road Network Topology Connectivity

This measure can effectively increase the density of drainage inlets and improve the runoff efficiency to flow to the underground drainage system. The number of roads per unit area in different catchments was significantly uneven, particularly in the lower Manhattan downtown area and the northern catchments of the Queens area, where road density was much higher than in other regions. This uneven spatial distribution posed challenges in achieving an efficient centralization of urban infrastructure, as the road network was often not highly connected. We proposed two recommendations (Figure 6): (1) Planning compact communities as opposed to urban sprawl, which could lead to a more connected road network and a more balanced distribution of urban infrastructure; (2) Designing a more human-scale road network structure to better coordinate road network planning with multiple design co-benefits, such as enhancing walkability and improving the sense of community.

- Increasing Average Road Width while Controlling Total Road Area

Increasing road width while controlling total road area can improve the surface runoff capacity of roads without increasing the impervious paving area. We found in Lower Manhattan's downtown area, the

northern and southeastern parts of Queens, and Staten Island, the average road width (3m to 10m) was significantly lower than in other areas. Consequently, these catchments' surface runoff capacity was lower than surrounding catchments. We proposed two suggestions in road network planning to address this issue (Figure 6). (1) Merging narrow and redundant roads to the adjacent roads to form wider roads; (2) Designing roadside green stormwater infrastructure (e.g., bioretention, biofiltration) to increase runoff infiltration capacity while controlling the impervious paving area constantly.

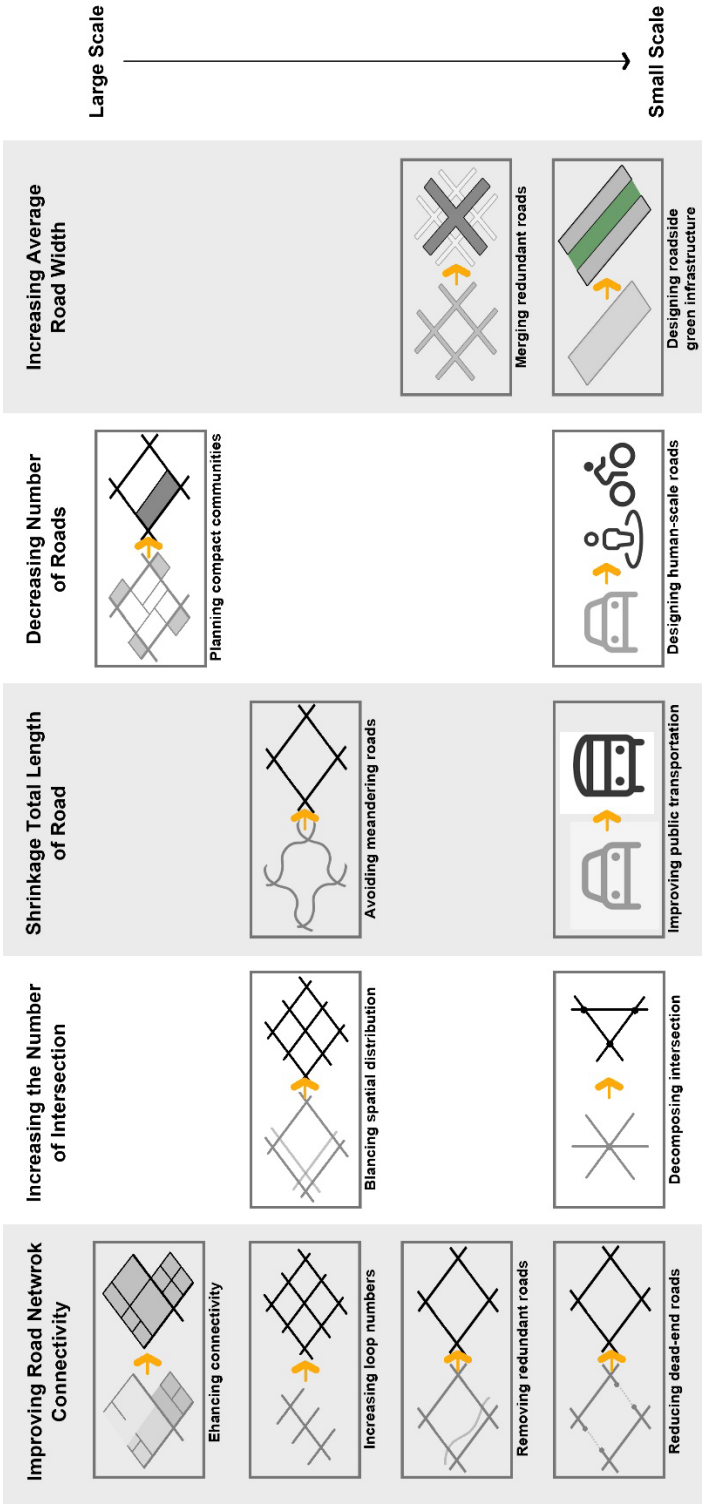

Figure 6. Road network planning suggestions

4.5. Limitations

The major limitation of this research is the bias in social media big data—the NYC 311 complaints data were limited by resident participation. Increasing residents' awareness regarding the flooding event report, especially when there is a forecasted precipitation would facilitate future modeling endeavors (Agonafir et al., 2022). In addition, the resident participation rate in reporting flooding varied in different regions due to the differences in complaint behavior and habits. For example, Staten Island has the most complaints per 10,000 residents, which was roughly double the complaints of Queens as the second highest frequently reported region (Agonafir et al., 2022). In addition, we excluded some areas for the road network topology calculation. We removed overpass and under tunnel from road network shapefile since the DEM did not accurately represent their elevation; We also excluded the direct storm drainage catchment because the sewer drainage type of Staten land had some errors. The omission of these areas and features could lead to a biased estimation of road network topology effect on street flooding.

Our regression models had several limitations. First, the spatial correlation of sewer catchments was not fully represented in GLMM regression because we did not incorporate the upstream and downstream relationships in the model. Second, there was no clear mechanism support of our model without testing it with a physical-based hydrological model. Third, some social factors were omitted because of data availability while they also affected the pattern in complaint reporting. Lastly, the regression model assumption was road network topology did not change drastically in this region during past 12 years, but this assumption might not hold for all regions in NYC.

Chapter 5 Conclusion

In recent years, crowd-sourcing data has become an effective tool for scientists to access flooding data due to rapid technological advancements and the widespread use of social media (Agonafir et al., 2022). While previous studies have examined the relationship between road networks and urban flooding, this study combined street flooding complaints with road network topology factors at a city scale. The results showed that road network connectivity significantly influenced street flooding risk, with Alpha having a negative effect and Beta, Theta having a positive effect on street flooding risk. The study concluded that road network topology connectivity was an influential factor in street flooding risks, while the impervious surface percentage was not. To mitigate street flooding in New York City, the study proposed five urban planning suggestions based on road network topology, such as enhancing road network connectivity, increasing the number of intersections, shrinking the total length of the road network, decreasing the number of roads, and increasing the average road width. These flooding mitigation strategies should be integrated into urban and transportation planning to promote a more resilient, healthy, and sustainable city.

Bibliography

Agonafir, C., Pabon, A. R., Lakhankar, T., Khanbilvardi, R., & Devineni, N. (2022). Understanding New York City street flooding through 311 complaints. *Journal of Hydrology*, *605*, 127300. https://doi.org/10.1016/j.jhydrol.2021.127300

Ahmed, K. R., & Akter, S. (2017). Analysis of landcover change in southwest Bengal delta due to floods by NDVI, NDWI and K-means cluster with landsat multi-spectral surface reflectance satellite data. *Remote Sensing Applications: Society and Environment*, *8*, 168–181. https://doi.org/10.1016/j.rsase.2017.08.010

Blumensaat, F., Wolfram, M., & Krebs, P. (2012). Sewer model development under minimum data requirements. *Environmental Earth Sciences*, *65*(5), 1427–1437. https://doi.org/10.1007/s12665-011-1146-1

Britain, G., & Brown, R. (2014). *Transport Resilience Review: A review of the resilience of the transport network to extreme weather events*. HM Government.

Butler, D., & Memon, F. A. (1999). Dynamic modelling of roadside gully pots during wet weather. *Water Research*, *33*(15), 3364–3372. https://doi.org/10.1016/S0043-1354(99)00050-0

Carleton, M. G. (1990). Comparison of Overflows from Separate and Combined Sewers – Quantity and Quality. *Water Science and Technology*, *22*(10–11), 31–38. https://doi.org/10.2166/wst.1990.0285

CEN. (1996). *Drain and sewer systems outside buildings–Part 2: Performance Requirements, European Standard, European Committee for Standardization CEN*.

Chang, H., & Franczyk, J. (2008). Climate Change, Land-Use Change, and Floods: Toward an Integrated Assessment. *Geography Compass*, *2*(5), 1549–1579. https://doi.org/10.1111/j.1749-8198.2008.00136.x

Chen, X.-Z., Lu, Q.-C., Peng, Z.-R., & Ash, J. E. (2015). Analysis of Transportation Network Vulnerability under Flooding Disasters. *Transportation Research Record*, *2532*(1), 37–44. https://doi.org/10.3141/2532-05

Chen, Y., Xu, Y., & Yin, Y. (2009). Impacts of land use change scenarios on storm-runoff generation in Xitiaoxi basin, China. *Quaternary International*, *208*(1), 121–128. https://doi.org/10.1016/j.quaint.2008.12.014

Cox, D., Hunt, J., Mason, P., Wheater, H., Wolf, P., Cox, D. R., Isham, V. S., & Northrop, P. J. (2002). Floods: Some probabilistic and statistical approaches. *Philosophical Transactions of the Royal Society of London. Series A: Mathematical, Physical and Engineering Sciences*, *360*(1796), 1389–1408. https://doi.org/10.1098/rsta.2002.1006

de Almeida, G. a. m., Bates, P., & Ozdemir, H. (2018). Modelling urban floods at submetre resolution: Challenges or opportunities for flood risk management? *Journal of Flood Risk Management*, *11*(S2), S855–S865. https://doi.org/10.1111/jfr3.12276

Ding, M., & Wei, Y. (2022). A conceptual framework for quantitatively understanding the impacts of floods/droughts and their management on the catchment's social-ecological system (C-SES). *Science of The Total Environment*, *828*, 154041. https://doi.org/10.1016/j.scitotenv.2022.154041

Dottori, F., Di Baldassarre, G., & Todini, E. (2013). Detailed data is welcome, but with a pinch of salt: Accuracy, precision, and uncertainty in flood inundation modeling. *Water Resources Research*, *49*(9), 6079–6085. https://doi.org/10.1002/wrcr.20406

Dubey, A. K., Gupta, U., & Jain, S. (2018). Comparative Study of K-means and Fuzzy C-means Algorithms on The Breast Cancer Data. *International Journal on Advanced Science, Engineering and Information Technology*, *8*(1), 18. https://doi.org/10.18517/ijaseit.8.1.3490

Edwards, A. W. F., & Cavalli-Sforza, L. L. (1965). A Method for Cluster Analysis. *Biometrics*, *21*(2), 362–375. https://doi.org/10.2307/2528096

Fewtrell, T. J., Duncan, A., Sampson, C. C., Neal, J. C., & Bates, P. D. (2011). Benchmarking urban flood models of varying complexity and scale using high resolution terrestrial LiDAR data. *Physics and Chemistry of the Earth, Parts A/B/C*, *36*(7), 281–291. https://doi.org/10.1016/j.pce.2010.12.011

Fowler, H. J., Blenkinsop, S., & Tebaldi, C. (2007). Linking climate change modelling to impacts studies: Recent advances in downscaling techniques for hydrological modelling. *International Journal of Climatology*, *27*(12), 1547–1578. https://doi.org/10.1002/joc.1556

Fox, D. M., Witz, E., Blanc, V., Soulié, C., Penalver-Navarro, M., & Dervieux, A. (2012). A case study of land cover change (1950–2003) and runoff in a Mediterranean catchment. *Applied Geography*, *32*(2), 810–821. https://doi.org/10.1016/j.apgeog.2011.07.007

Freiria, S., Ribeiro, B., & Tavares, A. O. (2015). Understanding road network dynamics: Link-based topological patterns. *Journal of Transport Geography*, *46*, 55–66. https://doi.org/10.1016/j.jtrangeo.2015.05.002

Gao, B. (1996). NDWI—A normalized difference water index for remote sensing of vegetation liquid water from space. *Remote Sensing of Environment*, *58*(3), 257–266. https://doi.org/10.1016/S0034-4257(96)00067-3

GISGeography. (2017, May 9). *What is NDVI (Normalized Difference Vegetation Index)?* GIS Geography. https://gisgeography.com/ndvi-normalized-difference-vegetation-index/

Gómez, M., & Russo, B. (2011). Methodology to estimate hydraulic efficiency of drain inlets. *Proceedings of the Institution of Civil Engineers - Water Management*, *164*(2), 81–90. https://doi.org/10.1680/wama.900070

Guo, R., Xin, C., Lin, P.-S., & Kourtellis, A. (2017). Mixed Effects Logistic Model to Address Demographics and Neighborhood Environment on Pedestrian Injury Severity. *Transportation Research Record*, *2659*(1), 174–181. https://doi.org/10.3141/2659-19

Hailegeorgis, T. T., & Alfredsen, K. (2017). Analyses of extreme precipitation and runoff events including uncertainties and reliability in design and management of urban water infrastructure. *Journal of Hydrology*, *544*, 290–305. https://doi.org/10.1016/j.jhydrol.2016.11.037

Hammond, M. J., Chen, A. S., Djordjević, S., Butler, D., & Mark, O. (2015). Urban flood impact assessment: A state-of-the-art review. *Urban Water Journal*, *12*(1), 14–29. https://doi.org/10.1080/1573062X.2013.857421

Hoekstra, A. Y., Buurman, J., & Ginkel, K. C. H. van. (2018). Urban water security: A review. *Environmental Research Letters*, *13*(5), 053002. https://doi.org/10.1088/1748-9326/aaba52

Kadaverugu, A., Gorthi, K. V., & Chintala, N. R. (2021). Impacts of Urban Floods on Road Connectivity—A Review and Systematic Bibliometric Analysis. *Current World Environment*, *16*(2), 575–593. https://doi.org/10.12944/CWE.16.2.22

Kalantari, Z., Nickman, A., Lyon, S. W., Olofsson, B., & Folkeson, L. (2014). A method for mapping flood hazard along roads. *Journal of Environmental Management*, *133*, 69–77. https://doi.org/10.1016/j.jenvman.2013.11.032

Kansky, K. J. (n.d.). *Structure of Transportation Networks: Relationships Between Network Geometry and Regional Characteristics* [Ph.D., The University of Chicago]. Retrieved March 31, 2023, from https://www.proquest.com/docview/302152135/citation/4556CDF2FFB84082PQ/1

Kramer, M., Terheiden, K., & Wieprecht, S. (2016). Safety criteria for the trafficability of inundated roads in urban floodings. *International Journal of Disaster Risk Reduction*, *17*, 77–84. https://doi.org/10.1016/j.ijdrr.2016.04.003

Lee, J., Chung, G., Park, H., & Park, I. (2018). Evaluation of the Structure of Urban Stormwater Pipe Network Using Drainage Density. *Water*, *10*(10), Article 10. https://doi.org/10.3390/w10101444

Lee, S., Nakagawa, H., Kawaike, K., & Zhang, H. (2016). Urban inundation simulation considering road network and building configurations. *Journal of Flood Risk Management*, *9*(3), 224–233. https://doi.org/10.1111/jfr3.12165

Li, C., Liu, M., Hu, Y., Wang, H., Zhou, R., Wu, W., & Wang, Y. (2022). Spatial distribution patterns and potential exposure risks of urban floods in Chinese megacities. *Journal of Hydrology*, *610*, 127838. https://doi.org/10.1016/j.jhydrol.2022.127838

Lipeme Kouyi, G., Rivière, N., Vidalat, V., Becquet, A., Chocat, B., & Guinot, V. (2010). Urban flooding: One-dimensional modelling of the distribution of the discharges through cross-road intersections accounting for energy losses. *Water Science and Technology*, *61*(8), 2021–2026. https://doi.org/10.2166/wst.2010.133

Lu, Y., Qin, X. S., & Xie, Y. J. (2016). An integrated statistical and data-driven framework for supporting flood risk analysis under climate change. *Journal of Hydrology*, *533*, 28–39. https://doi.org/10.1016/j.jhydrol.2015.11.041

M G, S., Karuppanagounder, K., & Anjaneyulu, M. (2021). Urban Road Network and its Topology: Case Study of Calicut, India. *European Transport\Trasporti Europei*.

Maantay, J., & Maroko, A. (2009). Mapping urban risk: Flood hazards, race, & environmental justice in New York. *Applied Geography*, *29*(1), 111–124. https://doi.org/10.1016/j.apgeog.2008.08.002

Mair, M., Zischg, J., Rauch, W., & Sitzenfrei, R. (2017). Where to Find Water Pipes and Sewers?—On the Correlation of Infrastructure Networks in the Urban Environment. *Water*, *9*(2), Article 2. https://doi.org/10.3390/w9020146

Maksimović, Č., Prodanović, D., Boonya-Aroonnet, S., Leitão, J. P., Djordjević, S., & Allitt, R. (2009). Overland flow and pathway analysis for modelling of urban pluvial flooding. *Journal of Hydraulic Research*, *47*(4), 512–523. https://doi.org/10.1080/00221686.2009.9522027

Medicine, N. A. of S., Engineering, and, Studies, D. on E. and L., Board, W. S. and T., Affairs, P. and G., Events, P. on R., Resilience, and Extreme, & States, C. on U. F. in the U. (2019). *Framing the Challenge of Urban Flooding in the United States*. National Academies Press.

Merwade, V., Olivera, F., Arabi, M., & Edleman, S. (2008). Uncertainty in Flood Inundation Mapping: Current Issues and Future Directions. *Journal of Hydrologic Engineering*, *13*(7), 608–620. https://doi.org/10.1061/(ASCE)1084-0699(2008)13:7(608)

Moffa, P. E. (1997). *The Control and Treatment of Combined Sewer Overflows*. John Wiley & Sons.

Moftakhari, H. R., AghaKouchak, A., Sanders, B. F., Allaire, M., & Matthew, R. A. (2018). What Is Nuisance Flooding? Defining and Monitoring an Emerging Challenge. *Water Resources Research*, *54*(7), 4218–4227. https://doi.org/10.1029/2018WR022828

Neal, J., Schumann, G., Fewtrell, T., Budimir, M., Bates, P., & Mason, D. (2011). Evaluating a new LISFLOOD-FP formulation with data from the summer 2007 floods in Tewkesbury, UK. *Journal of Flood Risk Management*, *4*(2), 88–95. https://doi.org/10.1111/j.1753-318X.2011.01093.x

Paquier, A., & Bazin, P.-H. (2014). Estimating uncertainties for urban floods modelling. *La Houille Blanche*, *6*, 13–18. https://doi.org/10.1051/lhb/2014057

Pons, F. (2010). Hydraulic Study of the Marseille Vieux-Port River Basin. In *Practical Applications in Engineering* (pp. 165–181). John Wiley & Sons, Ltd. https://doi.org/10.1002/9781118557792.ch15

Porta, S., Crucitti, P., & Latora, V. (2006). The network analysis of urban streets: A dual approach. *Physica A: Statistical Mechanics and Its Applications*, *369*(2), 853–866. https://doi.org/10.1016/j.physa.2005.12.063

Pregnolato, M., Ford, A., Wilkinson, S. M., & Dawson, R. J. (2017). The impact of flooding on road transport: A depth-disruption function. *Transportation Research Part D: Transport and Environment*, *55*, 67–81. https://doi.org/10.1016/j.trd.2017.06.020

Rahman, M., Ningsheng, C., Mahmud, G. I., Islam, M. M., Pourghasemi, H. R., Ahmad, H., Habumugisha, J. M., Washakh, R. M. A., Alam, M., Liu, E., Han, Z., Ni, H., Shufeng, T., & Dewan, A. (2021). Flooding and its relationship with land cover change, population growth, and road density. *Geoscience Frontiers*, *12*(6), 101224. https://doi.org/10.1016/j.gsf.2021.101224

Remote sensing of impervious surfaces: A review. (n.d.). https://doi.org/10.1080/02757250109532436

Rosenzweig, B. R., McPhillips, L., Chang, H., Cheng, C., Welty, C., Matsler, M., Iwaniec, D., & Davidson, C. I. (2018). Pluvial flood risk and opportunities for resilience. *WIREs Water*, *5*(6), e1302. https://doi.org/10.1002/wat2.1302

Russo, B., Valentín, M. G., & Tellez-Álvarez, J. (2021). The Relevance of Grated Inlets within Surface Drainage Systems in the Field of Urban Flood Resilience. A Review of Several Experimental and Numerical Simulation Approaches. *Sustainability*, *13*(13), Article 13. https://doi.org/10.3390/su13137189

Schaeffer, R., Szklo, A. S., Pereira de Lucena, A. F., Moreira Cesar Borba, B. S., Pupo Nogueira, L. P., Fleming, F. P., Troccoli, A., Harrison, M., & Boulahya, M. S. (2012). Energy sector vulnerability to climate change: A review. *Energy*, *38*(1), 1–12. https://doi.org/10.1016/j.energy.2011.11.056

Schubert, J. E., & Sanders, B. F. (2012). Building treatments for urban flood inundation models and implications for predictive skill and modeling efficiency. *Advances in Water Resources*, *41*, 49–64. https://doi.org/10.1016/j.advwatres.2012.02.012

Serrano, S. E., & Serrano, S. E. (2010). *Hydrology for engineers, geologists, and environmental professionals: An integrated treatment of surface, subsurface, and contaminant hydrology* (2nd ed., completely rev.). HydroScience Inc.

Sewer System—NYC DEP. (n.d.). Retrieved March 31, 2023, from https://www.nyc.gov/site/dep/water/sewer-system.page

Singh, P., Sinha, V. S. P., Vijhani, A., & Pahuja, N. (2018). Vulnerability assessment of urban road network from urban flood. *International Journal of Disaster Risk Reduction*, *28*, 237–250. https://doi.org/10.1016/j.ijdrr.2018.03.017

Smith, B., & Rodriguez, S. (2017). Spatial Analysis of High-Resolution Radar Rainfall and Citizen-Reported Flash Flood Data in Ultra-Urban New York City. *Water*, *9*(10), Article 10. https://doi.org/10.3390/w9100736

Smith, J. A., Baeck, M. L., Morrison, J. E., Sturdevant-Rees, P., Turner-Gillespie, D. F., & Bates, P. D. (2002). The regional hydrology of extreme floods in an urbanizing drainage basin. *Journal of Hydrometeorology*, *3*(3), 267–282.

Sytsma, A., Bell, C., Eisenstein, W., Hogue, T., & Kondolf, G. M. (2020). A geospatial approach for estimating hydrological connectivity of impervious surfaces. *Journal of Hydrology*, *591*, 125545. https://doi.org/10.1016/j.jhydrol.2020.125545

The Impact of Investing—NYW. (n.d.). Retrieved March 31, 2023, from https://www.nyc.gov/site/nyw/investing-in-nyw-bonds/the-impact-of-investing.page

Turner-Gillespie, D. F., Smith, J. A., & Bates, P. D. (2003). Attenuating reaches and the regional flood response of an urbanizing drainage basin. *Advances in Water Resources*, *26*(6), 673–684. https://doi.org/10.1016/S0309-1708(03)00017-4

Wang, R.-Q. (2018). Big Data of Urban Flooding: Dance with Social Media, Citizen Science, and Artificial Intelligence. *EGU General Assembly Conference Abstracts*, 404.

Wang, R.-Q., Mao, H., Wang, Y., Rae, C., & Shaw, W. (2018). Hyper-resolution monitoring of urban flooding with social media and crowdsourcing data. *Computers & Geosciences*, *111*, 139–147. https://doi.org/10.1016/j.cageo.2017.11.008

Wilson, J. N., Gader, P., Lee, W.-H., Frigui, H., & Ho, K. C. (2007). A Large-Scale Systematic Evaluation of Algorithms Using Ground-Penetrating Radar for Landmine Detection and Discrimination. *IEEE Transactions on Geoscience and Remote Sensing*, *45*(8), 2560–2572. https://doi.org/10.1109/TGRS.2007.900993

Wolff, C. G., & Burges, S. J. (1994). An analysis of the influence of river channel properties on flood frequency. *Journal of Hydrology*, *153*(1), 317–337. https://doi.org/10.1016/0022-1694(94)90197-X

Zhang, Y., Chen, Z., Zheng, X., Chen, N., & Wang, Y. (2021). Extracting the location of flooding events in urban systems and analyzing the semantic risk using social sensing data. *Journal of Hydrology*, *603*, 127053. https://doi.org/10.1016/j.jhydrol.2021.127053

Zope, P. E., Eldho, T. I., & Jothiprakash, V. (2016). Impacts of land use–land cover change and urbanization on flooding: A case study of Oshiwara River Basin in Mumbai, India. *CATENA*, *145*, 142–154. https://doi.org/10.1016/j.catena.2016.06.009